

STUDY ON OPTIMIZING MATERIALS FOR 3D GRIPPER PRINTING

Emilian Paduraru, Catalin Gabriel Dumitras, Dragos Florin Chitariu, Florin Chifan

“Gheorghe Asachi” Technical University of Iasi, Faculty of Mechanical Engineering and Industrial Management,
Blvd. Mangeron, No. 59A, 700050, Iasi, Romania

Corresponding author: Emilian Paduraru, emilian.paduraru@academic.tuiasi.ro

Abstract: The purpose of this paper is to identify the material that offers optimal characteristics in terms of cost, strength and weight. This is necessary because more and more composite materials and 3D printing are being used in the construction of robots, including the gripper. In this context, two types of materials are considered possible to be used in the construction of grippers. Samples are made in different 3D printing modes; the Taguchi method is applied to identify the optimal values. A finite element analysis was also performed in order to verify the characteristics of the materials introduced in the program by comparison with the experimental results in order to use them in the analysis of a new gripper solution. As they will follow, PLA material with 100% infill, 0,17mm layers thickness and 45° raster angle has the greatest resistance at extension. This material definition will be used in future research to the entire model of the gripper to see the behavior in different conditions given by the current requirements.

Key words: FDM, optimization, gripper printing.

1. INTRODUCTION

The Industrial robots are found in many industries around the world and serve a lot of different purpose, from heavy industry to food and medical industry. This means that a large variety of robot and effectors are necessary to serve those purpose. So, finding a gripper that is suitable to handle lots of parts with different geometries and dimensions can be difficult. Grippers are used for clamping various parts during handling, processing, control and assembly [1].

In this paper is presented one design solution and how to use 3D printing technologies to manufacture a complete gripper construction and more important how to determine different parameters for 3D printing in order to fulfill the proposed scope for the gripper.

In general, the gripper construction has rigid kinematic construction and therefore reduced flexibility but high clamping force [2].

The proposed solution presented in this paper has the main advantage of high level of configurability and it can be used for gripping of various different sizes and geometry shapes on the interior or exterior of the part.

The 3D model of the new gripper design is presented in Figure 1. The prehension mechanism consist in 4 fingers/ jaws with parallel open-close action to ensure a controllable contact with parts. The principle of operation of this gripping system is shown in Figure 2. When the pressurized air enters the pneumatic cylinder, it moves the piston which is connected by joints to the fingers of the system, making them close and implicitly perform an external grip of the part or release of the part in case of an external grip (Figure 2a). By introducing pressurized air to the other side of the cylinder, the fingers of the gripping system open to release the part or to make an internal grip of the part (Figure 2b).

The main function of this grip system is the possibility of folding the fingers, transforming from a grip system with four jaws in to a griping system with two jaws. The main advantage of this folding configuration is that it offers the possibility of gripping longer parts (i.e., shafts, sheet metals), making it a very flexible grip system. The angular movement of these fingers is done with the help of a separate pneumatic cylinder, which his only role is changing the grip system from one with four fingers to one with two and vice versa. Figure 3 shows the operation of the four-finger initial folding mechanism (Figure 1) for moving to the two-finger position. This second cylinder is connected to a ring which in turn is connected trough linkages to the fingers. When the pressured air entered in the right chamber (see Figure 3 – left) the ring is pushed and the folding from four to two finger gripper and vice versa, when the pressured air is entered in the left chamber it unfolds the fingers. Figure 3 (middle) shows by arrows the folding movement.

2. MATERIALS AND METHODS

2.1 3D printing

There are many 3D printing methods, such as Stereolithography (SLA), Selective Laser Sintering (SLS), Fused Deposition Modeling (FDM), Digital Light Process (DLP), Multi Jet Fusion (MJF),

PolyJet, Direct Metal Laser Sintering (DMLS), Electron Beam Melting (EBM) [3]. All of the

presented 3D printing methods can be used for creating the proposed gripper solution.

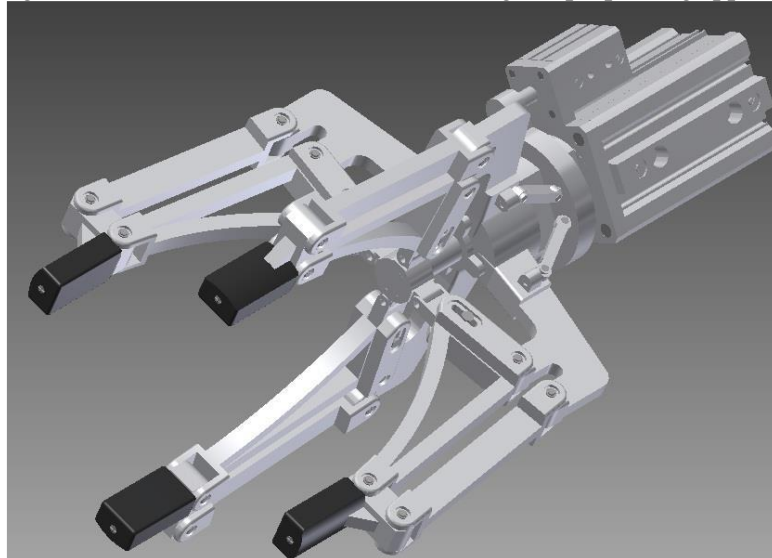


Fig. 1. 4-finger robot gripper solution

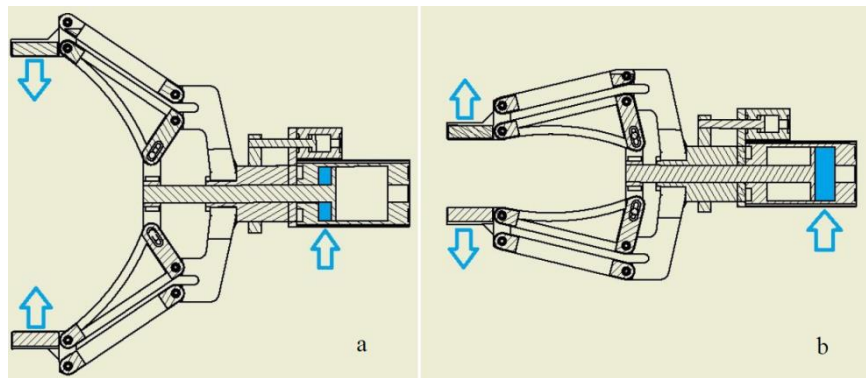


Fig. 2. Opening-closing principle using a pneumatic cylinder (a – closing; b – opening)

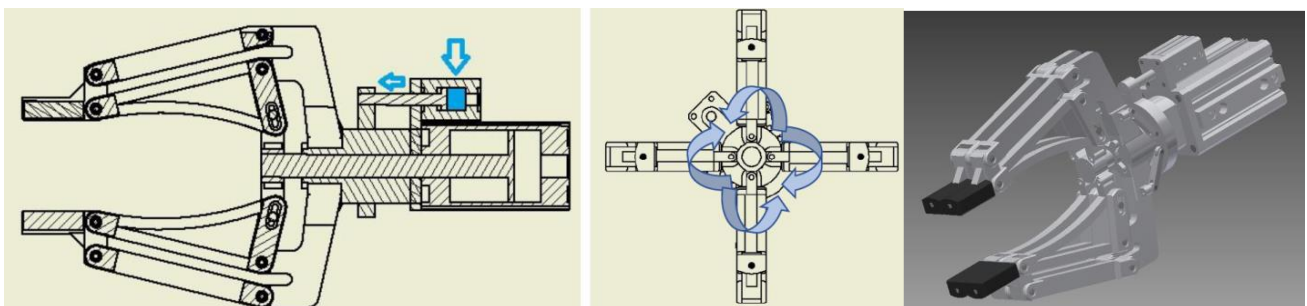


Fig. 3. The switch principle between 2 and 4 finger design

For this paper Fused Deposition Modeling (FDM) was used. This technology came out as an easy and progressive way to make the products and fast tooling of complicated components which are made in various batches. Researchers are experimenting and finding various types of material that can be used in the process [4 - 7]. In Figure 4 is represented a schematic diagram of the FDM Printer.

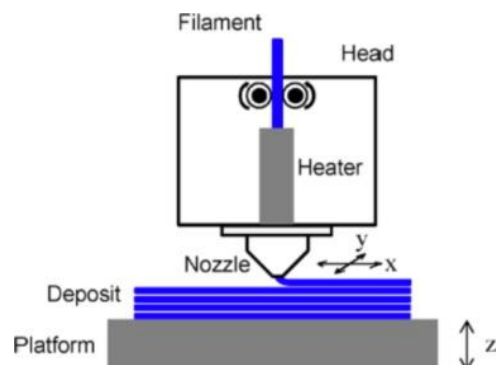


Fig. 4. A Schematic Diagram of FDM [7]

2.1 Work methodology

In order to correctly evaluate the behavior of the proposed gripper solution, a Finite Element Analysis can easily be used. But, arises the problem of determining the correct behavior of the material used for the 3D printing of the parts that composed the assembled gripper.

A standardized method for determining the behavior of the material must be used for testing different materials and infill parameters for the proposed specimens. The standardized dimensions for the specimen are selected from D638-14 Standard [8]. In Figure 5 is presented the shape of specimens and in Table 1 were shown the dimensions according to standard.

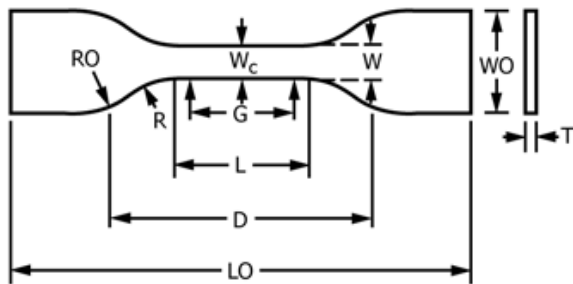


Fig. 5. Specimen geometry [6]

Table 1. Specimen Dimensions for Thickness, T, mm [6]

Dimensions	Type IV specimen [mm]
W—Width of narrow section	6
L—Length of narrow section	33
WO—Width overall, min	19
LO—Length overall, min	115
G—Gage length	25
D—Distance between grips	65
R—Radius of fillet	14
RO—Outer radius	25

2.2 Work methodology

A Taguchi method was used in order to determine the optimal solution for the printing of the parts. Various parameters were used for PLA and ABS material.

Taguchi method is a great technique to optimize the performance of products and process. By applying a systematic application of statistical experimental design which called robust design the variability around the target value of product proprieties is reduced. This robust design is an important technique for manufacturability and the life of a product. Taguchi simplified the usage of orthogonal arrays to setup experimental design [9].

In our test 3 different representative parameters were selected:

- Infill percentage: 60% and 100% (Figure 6);
- Raster angle: 45° and 90° (Figure 7);
- Layers thickness: 0.17 mm and 0.33 mm (Figure 8).

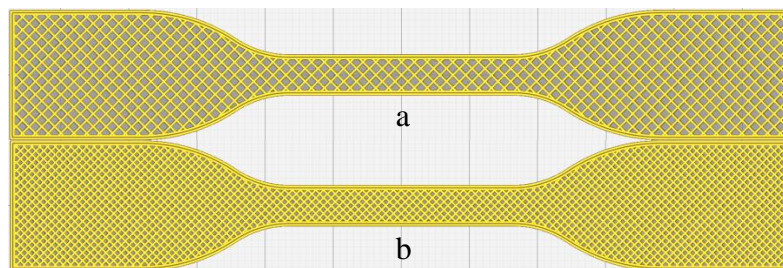


Fig. 6. Infill percentage (a – 60%, b – 100%)

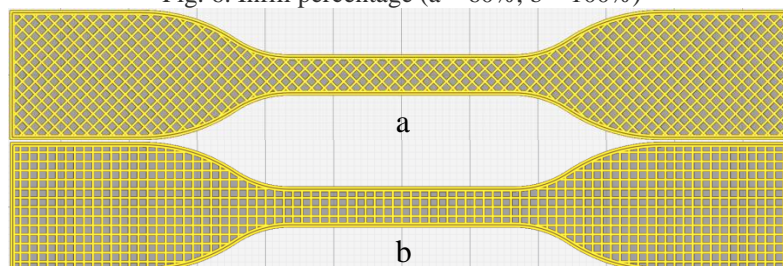


Fig. 7. Raster angle (a – 45°, b – 90°)

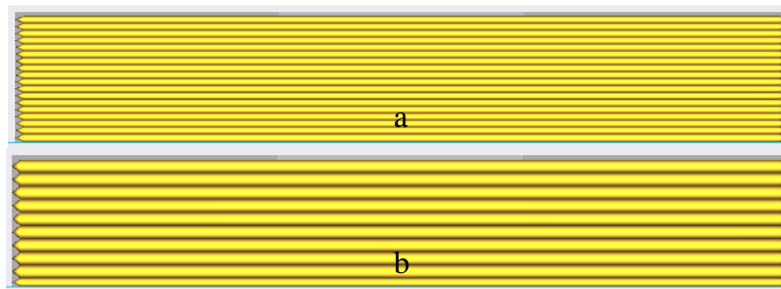


Fig. 8. Layers thickness (a – 0.17mm, b – 0.33mm)

Table 2. Design Table (randomized)

StdOrder	RunOrder	CenterPt	Blocks	Infill percentage	Layers thickness	Raster angle
7	1	1	1	60	0.33	90
1	2	1	1	60	0.17	45
4	3	1	1	100	0.33	45
3	4	1	1	60	0.33	45
6	5	1	1	100	0.17	90
2	6	1	1	100	0.17	45
8	7	1	1	100	0.33	90
5	8	1	1	60	0.17	90

Introducing these 3 parameters, each with 2 values, into a software to randomize and export all combinations, the results could be found in table below.

For conclusive and accurate results, each of the 8 types of specimens was printed in 3 copies. Also, for a comparison an even more conclusive result, two types of materials were used: Polylactic acid (PLA) and Acrylonitrile butadiene styrene (ABS). All of the specimens are shown in the Figure 9 (PLA in black color and ABS in blue color).

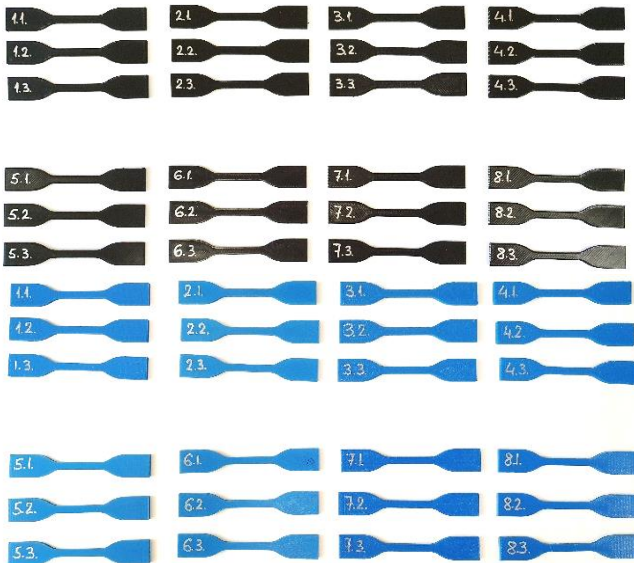


Fig. 9. 3D printed test specimens

All specimens were tested on an extension-compression testing equipment from Lloyd Instrument (Figure 10a) with a load cell of 5 kN at

room temperatures. The maximum load of each gripper is 2.5 kN). Test speed was 5 mm/min. The distance between the grippers is standardized (65 mm in this case) and is shown in Figure 10b.

3. RESULTS AND DISCUSSION

In these experiments were tested 8 types of printing processes with different combinations (the combination for each specimen can be found in Table 2), each of these 8 types were for two different materials (PLA and ABS). More than that, for all 16 specimen's types were made 3 copies for a total of 48 tensile tests. In Figures 11 and 12 each curve represents an average curve resulted from all 3 copies (i.e., in Figure 11 the curve named "1PLA" is an average curve between specimens 1.1, 1.2 and 1.3 – see Figure 9) and this is valid for each curve.

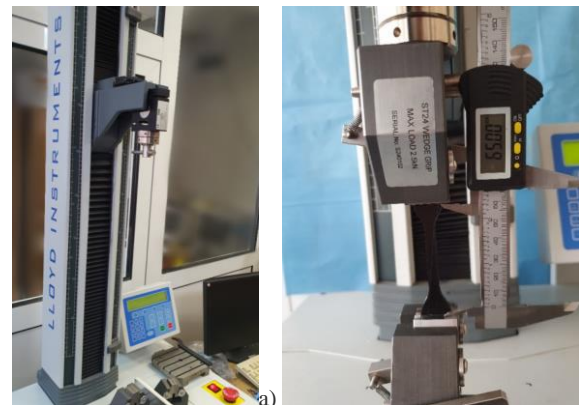


Fig. 10. Testing equipment (a – general view of machine; b – gripped specimen and the distance between grippers)

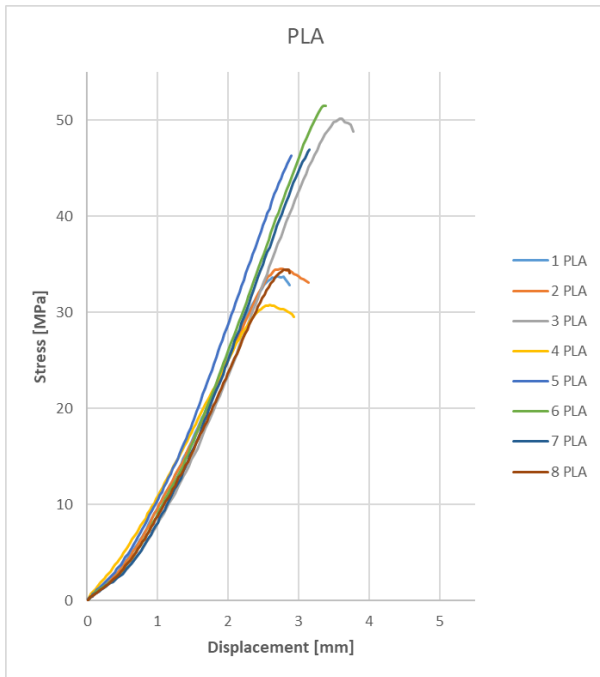


Fig. 11. Stress – displacement diagram for PLA specimens

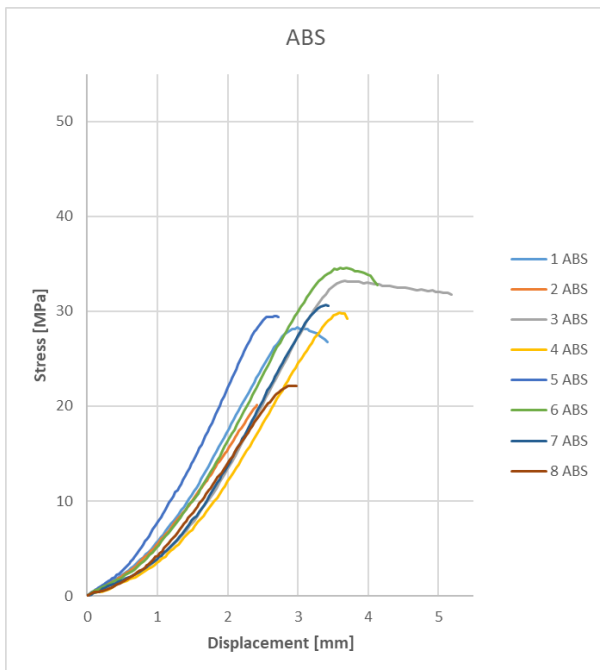


Fig. 12. Stress – displacement diagram for ABS specimens

Analyzing these two graphs (Figure 11 and 12) it can be observed that the most resistant material is the PLA material with 100% infill, 0,17mm layers thickness and 45° raster angle (green line or “6 PLA in Figure 11). This material was selected to convert it from a stress-displacement curve into a stress-strain curve material to enter it in Ansys software.

Based on the experimental results presented using Minitab software the Regression Equation was determined resulting the following regression eq. for PLA and ABS [10].

Regression Equation for PLA

$$\text{Yield} = 13.81 + 0.3833 \text{ Infill percentage} - 7.5 \text{ Layers thickness} - 0.0287 \text{ Raster angle} \quad (1)$$

The calculated R² indicator value for the model that provides indication if there is a good fit to the data has a value of R-sq = 95.71%.

Regression Equation for ABS:

$$\text{Yield} = 10.36 + 0.1766 \text{ Infill percentage} + 24.1 \text{ Layers thickness} - 0.0384 \text{ Raster angle} \quad (2)$$

The calculated R² indicator value for the model that provides indication if there is a good fit to the data has a value of R-sq = 92.49%.

The statistical analysis indicates that the proposed theoretical model for PLA is closer to the experimental values than the theoretical model for ABS.

3.1 Finite element analysis

In order to characterize the behavior of the 3D parts, a finite element analysis was performed, considering the experimental results obtained. Ansys 2022 software was used to perform the Finite Element Analysis.

In order to introduce the experimental results in the Finite Element Analysis the following steps were followed.

First, the Young’s Modulus need to be determined. To do this, a linear slope (represented with blue in Figure 13) is created and overlapped to the initial stress-displacement curve on a more linear section (represented with yellow in Figure 13) and extended to 0 on Y axis (blue dotted line). Then the initial curve is offset to the left until the blue dotted line reach 0 both X and Y axis (the red-dotted line on Figure 13). This step is important for Ansys software, since the initial curve from material test have a rounded bend at the beginning of the slope and the software need a straight line to define Young’s Modulus. For this material this Young’s Modulus is 1035 MPa. Looking closer to the curve it can be observed that at the end of the curve have a little bending. The bending begins at the Tensile Yield Strength of around 51 MPa and continues until the Tensile Ultimate Strength at around 51.5 MPa.

This little section from the end of the stress-displacement curve is the most challenging to made. After transforming the stress-displacement of the new curve (red dotted in Figure 13) into a stress-strain curve the next step was transforming this curve which is an engineering one into a true stress-strain curve.

In Finite Element Analysis stress-strain curve is used to determine the stress-displacement state of the tested specimen.

In order to correctly perform Finite Element Analysis in Ansys the Young’s Modulus values or the slope of the curve that is defined in the program needs to be

corrected in accordance with the experimental values. After determination of the curve that will go to Ansys program, the setup was done as shown in Figure 14. One side is fixed with a fix support and on the other side a displacement was applied.

For meshing it was used tetrahedrons method with linear element order resulting 9235 nodes and 41887 elements. This discretization could be observed in Figure 15.

Equivalent stress and directional deformation graph were considered and overlapped on the offset curve (see Figure 13 – green line).

Figure 15 presents the result on the specimen in Ansys software showing the areas where is the most predictable to break, and Figure 16 presents the breaking point of the specimen after the tensile test.

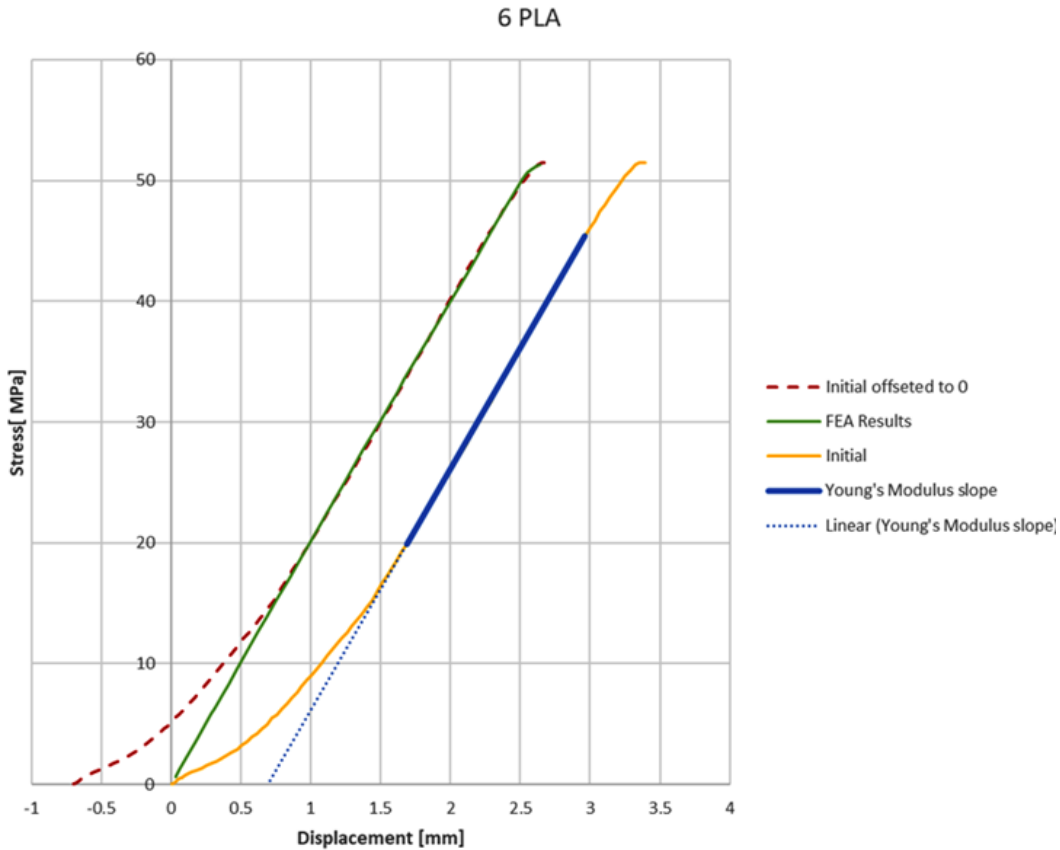


Fig. 13. Converting the stress-displacement curve, and the overlap of FEA with real test

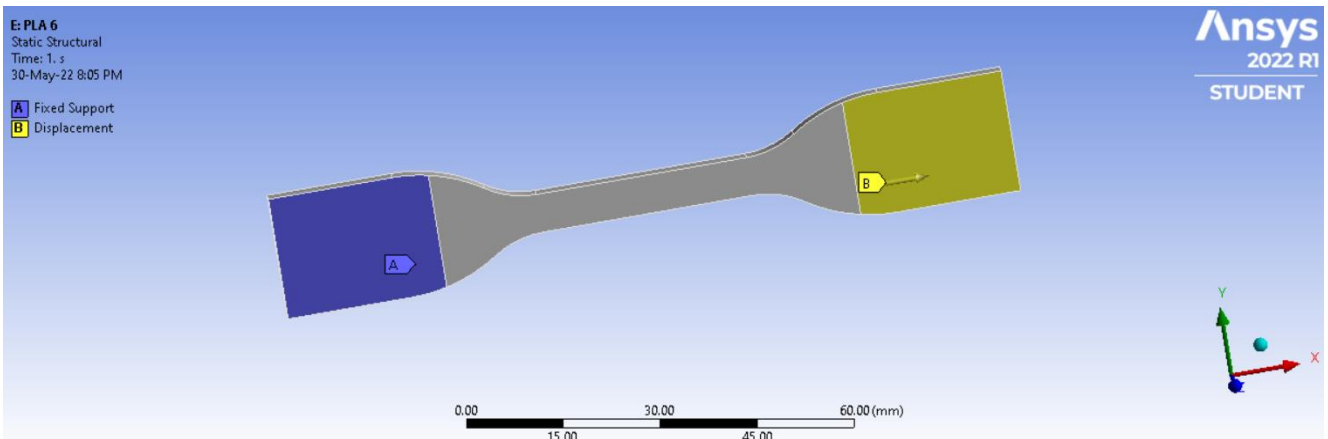


Fig. 14. Setup of the specimen on Ansys

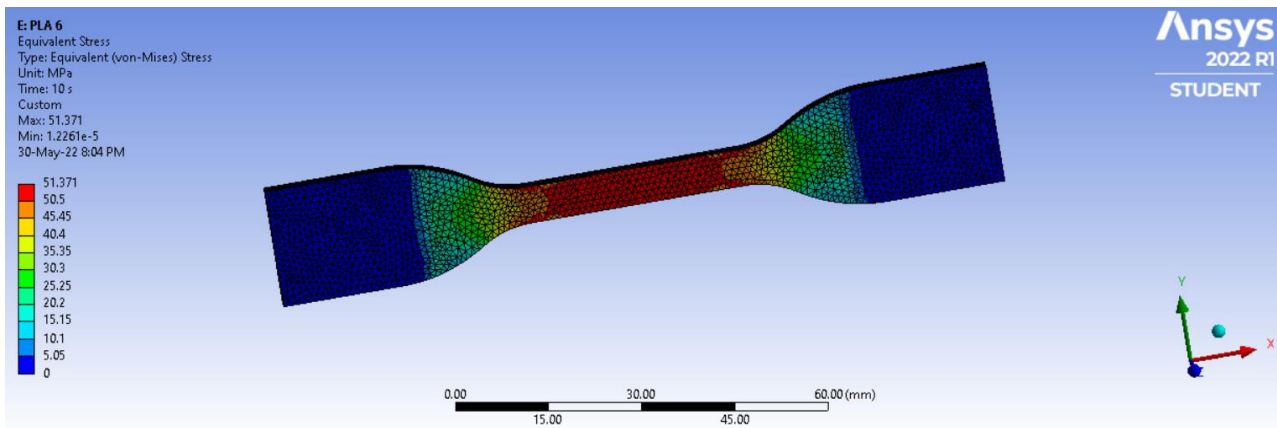


Fig. 15. FEA results on specimen (Ansys)



Fig. 16. Type 6 PLA specimens after tensile tests

The experimental results presented in Figure 13, after the testing of the specimen form Figure 16 are corresponding to the following values Young's Modulus: 1035 MPa, Tensile Yield Strength: around 51 MPa, Tensile Ultimate Strength: around 51.5 MPa.

4. CONCLUSIONS

The influence of the 3D printing parameters such as infill percentage, raster angle and layers thickness, influence the behavior of the final part. As it was observed, the PLA material with 100% infill, 0.17mm layers thickness and 45° raster angle has the greatest resistance at extension (presented in Figure 11 with green or "6PLA"). The strength is given by the infill percentage, since the 60% infill specimens brakes at considerably lower values (see "1PLA", "2PLA", "4PLA" and "8PLA" in Figure 11). Also, a great resistance is given by the raster angle of 45°.

Stress-displacement curve could be transformed in to a stress-strain one and introduced in Ansys software. Next step is to implement the defined material in to the full 3D model, to see the behavior of gripper.

The experimental results indicate that Young's Modulus, Tensile Yield Strength and Tensile Ultimate Strength are different that the considered values in Ansys standard database and requires corrections in order to be used in FEA. Once these parameters have been established, the FEA parameter can then be used on complex bodies such as the entire robot gripper describe at the beginning of this paper since the conventional resistance calculations are too difficult to implement.

5. REFERENCES

1. Chitariu, D.F., Paduraru, E., Dogan, G., Ilhan, M., Negoescu, F., Dumitras, C.G., Beznea, A., Stefanescu, V., Constantin, I., Berbece, S., Horodincea, M., (2020). *Experimental Research on Behavior of 3D Printed Gripper Soft Jaws*, Mater. Plast., 57(4), 366-375.
2. Monkman, G.J., Hesse, S., Steinmann, R., Schunk, H., (2006). *Robot Grippers* Wiley-VCH, Berlin.
3. Gebhardt, A., Hötter, J.S., (2016). *Additive Manufacturing 3D Printing for Prototyping and Manufacturing*, Carl Hanser Verlag, Munich.
4. Camargo, J.C., Machado, Á.R., Almeida, E.C., Silva, E.F.M.S., (2019). *Mechanical properties of PLA- graphene filament for FDM 3D printing*, Int. J. Adv. Manuf. Technol., 103(5–8), pp. 2423-2443.
5. Singh, S., Singh, R., (2017). *Integration of fused deposition modelling and vapor smoothing for biomedical applications*, Reference Module in Materials Science and Materials Engineering, pp. 1–15.
6. Boparai, K.S., Singh, R., (2019). *Development of rapid tooling using fused deposition modelling in Additive Manufacturing of Emerging Materials*, Springer International Publishing Cham, pp. 251-277.
7. Horvath, J., (2014). *A Brief History of 3D Printing*. In: *Mastering 3D Printing*, Apress, Berkeley, CA, https://doi.org/10.1007/978-1-4842-0025-4_1.
8. D638-14 Standard Test Method for Tensile Properties of Plastics.
9. Hamzaçebi, C., (2020). Taguchi Method as a Robust Design Tool, Available from: [10.5772/intechopen.94908](https://doi.org/10.5772/intechopen.94908).
10. Minitab, Available from: <https://support.minitab.com/>, Accessed on: 15/01/2022.

Received: July 21, 2022 / Accepted: December 15, 2022 / Paper available online: December 20, 2022 © International Journal of Modern Manufacturing Technologies